Am J Physiol Regul Integr Comp Physiol 289: R1202–R1211, 2005.
First published June 9, 2005; doi:10.1152/ajpregu.00816.2004.

Epithelial Ca^{2+} channel expression and Ca^{2+} uptake in developing zebrafish

Tien-Chien Pan,[1,2] Bo-Kai Liao,[1] Chang-Jen Huang,[1,3] Li-Yih Lin,[1] and Pung-Pung Hwang[1,2]

[1]*Institute of Cellular and Organismic Biology, Academia Sinica, Taipei;* [2]*Institute of Fisheries Science, National Taiwan University, Taipei; and* [3]*Institute of Biological Chemistry, Academia Sinica, Taipei, Taiwan, Republic of China*

Submitted 2 December 2004; accepted in final form 6 June 2005

Pan, Tien-Chien, Bo-Kai Liao, Chang-Jen Huang, Li-Yih Lin, and Pung-Pung Hwang. Epithelial Ca^{2+} channel expression and Ca^{2+} uptake in developing zebrafish. *Am J Physiol Regul Integr Comp Physiol* 289: R1202–R1211, 2005. First published June 9, 2005; doi:10.1152/ajpregu.00816.2004.—The purpose of the present work was to study the possible role of the epithelial Ca^{2+} channel (ECaC) in the Ca^{2+} uptake mechanism in developing zebrafish (*Danio rerio*). With rapid amplification of cDNA ends, full-length cDNA encoding the ECaC of zebrafish (zECaC) was cloned and sequenced. The cloned zECaC was 2,578 bp in length and encoded a protein of 709 amino acids that showed up to 73% identity with previously described vertebrate ECaCs. The zECaC was found to be expressed in all tissues examined and began to be expressed in the skin covering the yolk sac of embryos at 24 h postfertilization (hpf). zECaC-expressing cells expanded to cover the skin of the entire yolk sac after embryonic development and began to occur in the gill filaments at 96 hpf, and thereafter zECaC-expressing cells rapidly increased in both gills and yolk sac skin. Corresponding to ECaC expression profile, the Ca^{2+} influx and content began to increase at 36–72 hpf. Incubating zebrafish embryos in low-Ca^{2+} (0.02 mM) freshwater caused upregulation of the whole body Ca^{2+} influx and zECaC expression in both gills and skin. Colocalization of zECaC mRNA and the Na^+-K^+-ATPase α-subunit (a marker for mitochondria-rich cells) indicated that only a portion of the mitochondria-rich cells expressed zECaC mRNA. These results suggest that the zECaC plays a key role in Ca^{2+} absorption in developing zebrafish.

calcium influx; low calcium, mitochondria-rich cells; zebrafish embryo

THE ZEBRAFISH has a significant presence in developmental biology, where its scientific utility is well recognized. Increasingly, it is regarded as a useful model for the study of human diseases and vertebrate organogenesis as well as the functioning of whole organs or the entire organism (1, 3). The gills, skin, kidneys, and intestines are the major organs responsible for homeostasis of body fluid composition in fish. During the embryonic stages of fish, skin has long been suggested to be the major extrarenal region for regulating body fluid composition before the development of functional gills (2, 7, 13, 18, 19, 24–26, 42). The skin of zebrafish embryos and larvae is an excellent model to study the differentiation and function of vertebrate transport epithelia and their ionocytes, because it is comparatively easy to conduct morphological observations and functional assays on embryonic skin in vivo.

Ca^{2+} is a vital element for almost all animals, especially vertebrates, and levels in body fluids are maintained in a narrow range of ~2–3 mM. For terrestrial vertebrates, food is the main source of Ca^{2+}, and the intestines serve as a primary site for Ca^{2+} uptake. The situation for aquatic animals is fundamentally different. Fish are continuously exposed to waters with variable Ca^{2+} concentrations (seawater [Ca^{2+}], 10 mM; freshwater [Ca^{2+}], ~0.01–3 mM), and therefore it is critical for fish to control Ca^{2+} flow into or out of their bodies. In freshwater fish, the gills are the main site (>97% of the whole body) of Ca^{2+} uptake (9). Mitochondria-rich (MR) cells have long been known to be responsible for transcellular Ca^{2+} uptake in fish gills (9, 23, 31, 33, 37).

Fish embryos and larvae, whose gills or other osmoregulatory organs are poorly developed or underdeveloped, are able to absorb Ca^{2+} from freshwater environments probably via skin MR cells (21). In the case of tilapia, a euryhaline fish, Ca^{2+} content of the body and influx remain constant during embryonic development and show a rapid increase after hatching (21). Acclimation to low-Ca^{2+} freshwater causes the larvae of tilapia, goldfish, ayu, and zebrafish to raise the affinity and transport velocity of Ca^{2+} to fit their growth (5, 6).

Regarding the Ca^{2+} uptake mechanism of fish MR cells, Flik et al. (12) proposed a model, similar to that for Ca^{2+} reabsorption in the mammalian kidney (16), in which the basolateral plasma membrane Ca^{2+}-ATPase (PMCA) and Na^+/Ca^{2+} exchanger (NCX), as well as the cytosol Ca^{2+} binding protein and the apical Ca^{2+} channels (ECaCs), may be involved. Activities of PMCA and NCX, which extrude Ca^{2+} from the cytosol into the blood, were both found in basolateral membranes of fish gill cells (10–12), but the relative importance of the two transporters to the overall Ca^{2+} absorption process is unknown. Van der Heijden et al. (45) found that there was no significant difference in the activities and kinetics of either PMCA or NCX between sham control and stanniectomized eels. Considering the kinetic properties of PMCA and NCX, the extrusion mechanisms seemed to operate far below their maximum capacity in fish gills (10). According to the Ca^{2+} reabsorption model in the mammalian kidney (16), from an energetic standpoint, controlling Ca^{2+} influx in various environments with the ATP-consuming step (i.e., PMCA and NCX) may be too energy costly, and the entry of Ca^{2+} from water via the ECaC serves as the rate-limiting step. There has been no molecular evidence so far to support the involvement of the ECaC in Ca^{2+} uptake in fish MR cells, although stanniocalcin (a hypocalcemic hormone) and lanthanum (a voltage-independent Ca^{2+} channel blocker) have been shown to inhibit Ca^{2+} transport through apical membrane of fish gills (35), and Ca^{2+} uptake function was demonstrated recently in Madin-Darby canine kidney cells expressing the fugu ECaC (40).

The purpose of the present work was to study the involvement of the ECaC in the Ca^{2+} uptake mechanism in developing

Address for reprint requests and other correspondence: P. P. Hwang, Institute of Cellular and Organismic Biology, Academia Sinica, Taipei, Taiwan 11529, ROC (e-mail: pphwang@gate.sinica.edu.tw).

The costs of publication of this article were defrayed in part by the payment of page charges. The article must therefore be hereby marked "*advertisement*" in accordance with 18 U.S.C. Section 1734 solely to indicate this fact.

zebrafish. In the present study, the zebrafish ECaC (zECaC) was cloned, and the gene developmental expression and tissue distribution also were examined. Cellular localization of the zECaC was investigated using in situ hybridization to test whether the zECaC is expressed in MR cells. Changes in the Ca^{2+} content and Ca^{2+} influx during zebrafish embryogenesis were studied, and effects of environmental Ca^{2+} levels on the Ca^{2+} balance and ECaC expression also were examined.

MATERIALS AND METHODS

Animals. Zebrafish stocks were kept in local tap water at 28.5°C under a 14:10-h light-dark photoperiod at the Institute of Cellular and Organismic Biology, Taipei, Taiwan. Fish selected to breed were transferred into a breeding tank for collecting fertilized eggs. Embryos were collected within 30 min after fertilization and incubated in a beaker until the desired developmental stage [12, 24, 36, 48, 60, 72, 96, 120, 144, and 168 h postfertilization (hpf)] at 28.5°C. The experimental protocols were approved by the Academia Sinica Institutional Animal Care and Utilization Committee (approval no. RFiZOOHP2002086).

Preparation of total RNA. Zebrafish embryos and adults were anesthetized with buffered MS-222 (3-aminobenzoic acid ethyl ester, 100–200 mg/l; Sigma, St. Louis, MO), and then appropriate amounts of embryos and adult tissues were collected and homogenized in 4 ml of *solution D* (4 M guanidine thiocyanate, 1.25 M sodium citrate, 35% *N*-lauroylsarcosine sodium salt, and 0.1 M 2-mercaptoethanol). Tissue homogenates then were mixed with 0.4 ml of 2 M sodium acetate, 0.8 ml of choloroform-isopropanol (49:1), and 4 ml of phenol and thoroughly shaken. After centrifugation at 4°C and 12,000 *g* for 30 min, supernatants were obtained and mixed with an equal volume of isopropanol. Pellets were precipitated by another centrifugation at 4°C and 12,000 *g* for 30 min, washed with 70% alcohol, and stored at −20°C before use. The amount and quality of the total RNA were determined by measuring the absorbance at 260 and 280 nm with a spectrophotometer (U-2000; Hitachi, Tokyo, Japan) and an RNA denatured gel.

RT-PCR analysis. Total RNAs extracted from zebrafish tissues and embryos were treated with DNase I (Promega, Madison, WI) to remove DNA contamination. After DNase I digestion, phenol-chloroform extraction and purification were performed to stop the reaction. For cDNA synthesis, ~5–10 μg of total RNA were reverse-transcribed in a final volume of 20 μl containing 0.5 mM dNTPs, 2.5 μM oligo$(dT)_{20}$, 250 ng of random primers, 5 mM dithiothreitol, 40 units of RNase inhibitor, and 200 units of SuperScript III RT (Invitrogen, Carlsbad, CA) for 1 h at 50°C, followed by a 70°C incubation for 15 min. For PCR amplification, 4 μg of cDNA were used as template in a 50-μl final reaction volume containing 0.25 mM dNTPs, 2.5 units of Ex*Taq* polymerase (Takara, Shiga, Japan), and 0.2 μM of each primer. Thirty cycles were performed for each reaction. The primer sets in the PCR for the tissue scan and gene expression during developmental stages were, for the Ca^{2+} channel (a 295-bp fragment), forward 5′-GCTGCGAGTCACTGGAATA-3′ and reverse 5′-ACCGACGCTCACCTCAAACT-3′, and for β-actin (a 560-bp fragment), forward 5′-ACGCTTCTGGTCGTACTACTGGTATTGTGA-3′ and reverse 5′-GATCTTGATCTTCATGGTGGAAGGAGCAAG-3′. The amplicons all were sequenced to ensure that the PCR products were the desired gene fragments.

RNA probe synthesis. Three fragments of zebrafish ECaC (nucleotides 349–696, 982–1979, and 1840–2156) were obtained by PCR and inserted into the pGEM-T Easy vector (Promega). Purified plasmids were then linearized by restriction enzyme digestion, and in vitro transcription was performed with T7 and SP6 RNA polymerase (Roche, Penzberg, Germany), respectively, in the presence of digoxigenin (dig)-UTP (47). Dig-labeled RNA probes were examined with RNA gels and dot-blot assay (to confirm the quality and concentration). For dot-blot assay (Dig RNA labeling kit; Roche Diagnostics, Mannheim, Germany), the synthesized probes and the standard RNA probes were spotted on nitrocellulose membrane according to the manufacturer's instructions. After cross-linking and blocking, the membrane was incubated with an alkaline phosphatase-conjugated anti-dig antibody and stained with nitro blue tetrazolium (NBT) and 5-bromo-4-chloro-3-indolyl phosphate (BCIP).

Whole mount in situ hybridization. Zebrafish embryos, ~5–10 individuals for each stage, were anesthetized with buffered MS-222, fixed with 4% paraformaldehyde overnight at room temperature, and then washed several times with phosphate-buffered saline (PBS). Fixed samples were rinsed with PBST (0.2% Tween 20, 1.4 mM NaCl, 0.2 mM KCl, 0.1 mM Na_2HPO_4, and 0.002 mM KH_2PO_4; pH 7.4), treated with 50 μg/ml proteinase K for 5–20 min, washed with PBST several times, and then postfixed in 4% paraformaldehyde in PBS for 10 min. After a brief washing with PBST, slides were incubated with hybridization buffer (HyB) containing 60% formamide, 5× SSC, and 0.1% Tween 20 for 5 min at 65°C. Prehybridization was performed in HyB^+, which is the hybridization buffer supplemented with 500 μg/ml yeast tRNA and 50 μg/ml heparin (Sigma) for 2 h at 65°C. After prehybridization, samples were incubated in 100 ng of the RNA probe in 200 μl of HyB^+ at 65°C overnight for hybridization. Slides were then washed at 65°C for 10 min in 75% HyB and 25% 2× SSC, 10 min in 50% HyB and 50% 2× SSC, 10 min in 25% HyB and 75% 2× SSC, 10 min in 2× SSC, and two times for 30 min in 0.2× SSC at 70°C. Further washes were performed at room temperature for 5 min in 75% 0.2× SSC and 25% PBST, 5 min in 50% 0.2× SSC and 50% PBST, 5 min in 25% 0.2× SSC and 75% PBST, and 5 min in PBST. After serial washings, slides were incubated in blocking solution containing 5% sheep serum and 2 mg/ml BSA in PBST for 2 h and then incubated in 1:2,000 alkaline phosphatase-conjugated anti-dig antibody in blocking solution for another 2 h at room temperature. After the reaction, samples were washed with PBST plus blocking reagent and transferred to the staining buffer. The staining reaction was held with NBT and BCIP in staining buffer until the signal was sufficiently strong. Samples were observed with a stereomicroscope (SZX-ILLD100; Olympus, Tokyo, Japan) or an upright microscope (BX-50WI; Olympus), depending on the image size desired. Different embryonic stages of zebrafish were sampled for measuring the changes in zECaC-expressing cell density (cells/yolk sac) following development. For each individual, zECaC-expressing cells in one side of the yolk sac were counted. For samples of the acclimation experiment (see below), density (cells/4,900 μm^2), size, and mRNA signal intensity of zECaC-expressing cells in the gill region were measured. Images for the measurements were taken at the middle of the gill region (between the edges of eye and operculum; see Fig. 6, *E* and *F*) from the lateral side of fish head. A commercial image analysis program (Image-Pro Plus 4.0; Media Cybernetics, Silver Spring, MD) was used to measure surface area as cell size (μm^2) and the total intensity of the hybridization reaction as the mRNA level (arbitrary numerical value) in each cell, and the data from 15 cells were averaged for each individual.

Immunohistochemistry. After being anesthetized with buffered MS-222, zebrafish embryos were dechorionated and fixed in 4% paraformaldehyde for 10 min at 4°C. After being washed in PBS, fixed embryos were treated with 100% ethanol for 10 min at −20°C and subsequently subjected to blocking with 3% BSA at room temperature for 30 min. Embryos were then incubated with 1:100 PBS-diluted mouse anti-chicken Na^+/K^+-ATPase α-subunit (cytosolic epitope for all isoforms) monoclonal IgG (Developmental Studies Hybridoma Bank, University of Iowa, Iowa City, IA) at room temperature for 2 h. Samples were washed twice in PBS for 10 min each and then incubated with 1:200 PBS-diluted goat anti-mouse IgG conjugated with FITC (Jackson ImmunoResearch Laboratories, West Grove, PA) for 1 h at room temperature. Images were acquired with a confocal laser scanning microscope (TCS-NT; Leica Lasertechnik, Heidelberg, Germany) equipped with the BF 525/550 filter set for monitoring

FITC. For double labeling, some samples were subjected to ECaC in situ hybridization and then to Na^+/K^+-ATPase immunocytochemistry. Images of ECaC mRNA and Na^+/K^+-ATPase protein were merged with a computer.

Acclimation experiment. According to the method of Chen et al. (5), high-Ca^{2+} (2.00 mM, control) and low-Ca^{2+} (0.02 mM) artificial freshwaters were prepared with double-deionized water (Milli-RO60; Millipore, Billerica, MA) supplemented with adequate $CaSO_4 \cdot 2H_2O$, $MgSO_4 \cdot 7H_2O$, NaCl, K_2HPO_4, and KH_2PO_4. Ca^{2+} concentrations (total Ca^{2+} levels measured by absorption spectrophotometry, see *Measurement of whole body Ca^{2+} content*) of the high- and low-Ca^{2+} media were 2.0 and 0.02 mM, respectively, but the other ion concentrations of the three media were the same ($[Na^+]$, 0.5 mM; $[Mg^{2+}]$, 0.16 mM; $[K^+]$, 0.3 mM) as those in local tap water. Variations in the ion concentrations were maintained within 10% of the predicted values. Zebrafish fertilized eggs were transferred to high- and low-Ca^{2+} media, respectively, and incubated thereafter until sampling. At the end of acclimation (120 hpf), seven to nine embryos for each group were subjected to Ca^{2+} influx measurements and zECaC whole mount in situ hybridization.

Measurement of whole body Ca^{2+} content. Zebrafish embryos were anesthetized with MS-222, dechorionated, and briefly rinsed in deionized water, and 10 individuals were pooled as one sample. HNO_3 (13.1 N) was added to samples for digestion at 60°C overnight. Digested solutions were diluted with double-deionized water, and the total Ca^{2+} content was measured with an atomic absorption spectrophotometer (Z-8000; Hitachi). Standard solutions from Merck (Darmstadt, Germany) were used to make the standard curves.

Measurement of whole body Ca^{2+} influx. By following previously described methods (5) with some modifications, zebrafish embryos were dechorionated, rinsed briefly in deionized water, and then transferred to a 4-ml $^{45}Ca^{2+}$ (Amersham, Piscataway, NJ; final working specific activity, 1–2 mCi/mmol)-containing medium for a subsequent 4-h incubation. After incubation, embryos were washed several times in isotope-free water medium. Three embryos were pooled into one vial, anesthetized with MS-222, and then digested with tissue solubilizer (Solvable; Packard, Meriden, CT) at 50°C for 8 h. The digested solutions were supplemented with counting solution (Ultima Gold; Packard), and the radioactivities of the solutions were counted with a liquid scintillation beta counter (LS6500; Beckman, Fullerton, CA). The Ca^{2+} influx was calculated using the following formula:

$$J_{in} = Q_{embryo} X_{out}^{-1} t^{-1} W^{-1},$$

where J_{in} is the influx ($pmol \cdot mg^{-1} \cdot h^{-1}$), Q_{embryo} is the radioactivity of the embryo (cpm per individual) at the end of incubation, X_{out} is the specific activity of the incubation medium (cpm/pmol), t is the incubation time (h), and W is the average body wet weight of different stage embryos (mg).

Statistical analysis. Values are presented as the means ± SD and were compared using Student's *t*-test or one-way analysis of variance (ANOVA) (Tukey's pairwise comparison).

RESULTS

Identification and characterization of zECaC. Two zebrafish EST clones (accession nos. AL925143 and AW455111) encoding the ECaC were identified by searching the GenBank database. Specific primers were designed according to the sequence of these two EST clones, and full-length cDNA of the zECaC was cloned and sequenced. The total length of nucleotides was 2,578 bp with an open reading frame of 2,130 bp that encodes a protein of 709 amino acids (aa) (Fig. 1; accession no. NM001001849). The zECaC reveals six putative transmembrane domains (Fig. 1). In accordance with its mammalian counterparts, a hydrophobic pore region between transmembrane domains 5 and 6, as well as three ankyrin repeats, are conserved (Fig. 1). The length of the zECaC protein is shorter than that of mammals (723–729 aa) and trout (727 aa). The zECaC showed the highest amino acid sequence identity of 72–73% to the recently cloned rainbow trout (AY256348) and fugu (AY383562) ECaC. Moreover, the zECaC showed 53.2, 47.7, and 50.7% identities to Ca^{2+} transporter 1 (CaT1) of the human (AJ277909), mouse (AB037373), and rat (AF160798), respectively, and 51.4, 50.8, 50.5, and 48.1% identities to the ECaC of the human (AJ271207), mouse (XP149866), rabbit (AJ133128), and rat (AB032019), respectively. The lowest identity was 45% to CaT1 of *Xenopus laevis* (BAC24123). For the other members of the osm transient receptor potential channel (OTRPC) subfamily (VR1, VRL-1, VRL-2, VR-OAC, and SIC), an average of 30% identity was found.

As shown in Fig. 2, a phylogenetic tree was generated using the neighbor-joining analysis (5,000 replicates). The analysis included entire amino acid sequences of zebrafish, fugu, and trout ECaCs, mammalian ECaCs and CaT1s, and *Xenopus laevis* CaT1. The ECaCs were clustered into three groups. Two mammalian isoforms of the ECaC, ECaC and CaT1, were clustered into one group, whereas amphibian CaT1 and fish ECaCs were in two other groups, respectively.

zECaC expression patterns in zebrafish embryos and various tissues. Expression of the zECaC was evaluated by RT-PCR using total RNA extracted from 0- to 72-hpf zebrafish embryos. As shown in Fig. 3, a PCR product of the zECaC of 295 bp was first detected at 24 hpf, and the expression increased after development. The RT-PCR analysis was repeated with four different sets of samples, and the results were similar. In adult fish, zECaC expression was ubiquitous among tissues examined, including the brain, heart, gill, intestine, liver, and kidney. The higher expression level was found in the gill, whereas the lower level was in the liver. The relative levels of mRNA in the brain, heart, gill, intestine, liver, and kidney were 6.7 ± 1.8, 53.1 ± 10.0, 154.3 ± 74.0, 2.4 ± 0.5, 3.7 ± 3.1, and 11.0 ± 2.0, respectively ($n = 4$ individuals, β-actin as internal control).

Localization of zECaC mRNA in developing zebrafish. Observations of zECaC mRNA focused on the skin and gills, because these regions were previously reported to cover >97.4% of the extraintestinal Ca^{2+} uptake in fish (9). No significant signal of zECaC mRNA was found in the skin of embryos at 12 hpf. In 24-hpf embryos, zECaC mRNA was first found in the cells on the skin covering the yolk sac, but very few signals were found in the skin of somites (Fig. 4, *A* and *B*). zECaC-expressing cells expanded to cover the skin of the entire yolk sac after embryonic development (Fig. 4, *A*, *C*, and *D*) and began to occur in the branchial region at 72 hpf (Fig, 4, *C* and *D*). zECaC-expressing cells appeared in gill filaments at 96 hpf (Fig. 4*E*), and thereafter the cell numbers rapidly increased in both gills and yolk sac skin (Fig. 4, *E–G*). Further quantitative analysis of the density changes of zECaC-expressing cells after development was conducted in yolk sac, where most of the cells localized. The density of zECaC-expressing cells in yolk sac was increased ~4.5-fold from 24 to 120 hpf (Fig. 5). The negative control with the zECaC sense cRNA probe showed no signal of zECaC mRNA (data not shown).

zECaC mRNA also was found in the brain region at 24 hpf (Fig. 4*A*), but the signal was unclear in the same region at the later stages (Fig. 4, *C* and *F*), probably because the duration (or

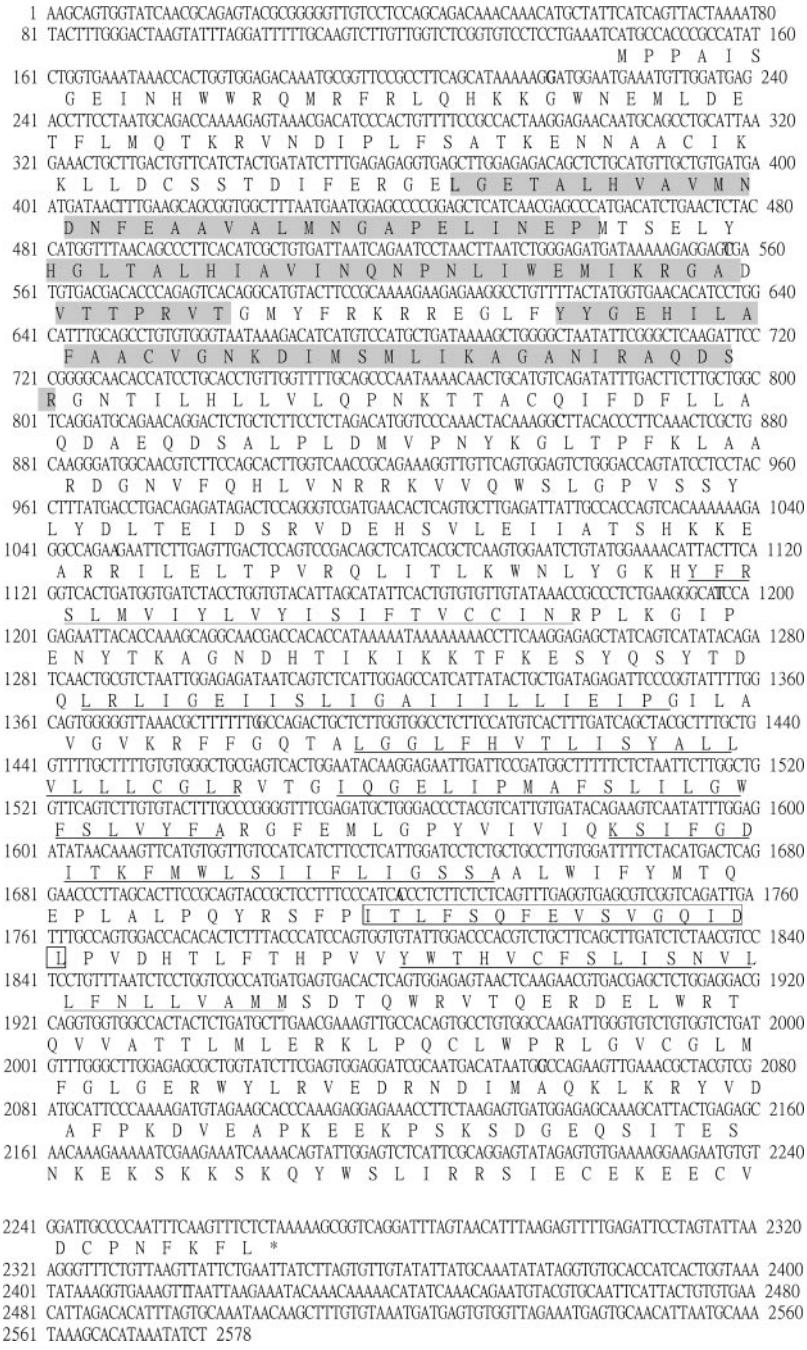

Fig. 1. Nucleotide and deduced amino acid sequence of zebrafish epithelial Ca^{2+} channel (ECaC) cDNA. Asterisk indicates the translational stop codon. Amino acid sequences for 3 ankyrin repeats (shaded), an ion pore region (open box), and 6 transmembrane domains (underlined) were postulated from the mammalian ECaC.

concentration) of proteinase K treatment was too short to allow the penetration of zECaC probes to the internal organs in zebrafish larvae.

Expression of zECaC mRNA in MR cells. MR cells, which were identified with the signal of the Na^+/K^+-ATPase protein (a marker for fish MR cells; Ref. 20), occurred initially in the body skin including the yolk sac skin of zebrafish embryos at 24 hpf (data not shown). The number of MR cells in the skin covering both somites and the yolk sac rapidly increased after embryonic development (Fig. 6, *A* and *B*). Double labeling of Na^+/K^+-ATPase and zECaC mRNA was conducted in embryos to certify whether MR cells express zECaC mRNA. Merged images of the signals of Na^+/K^+-ATPase and zECaC mRNA indicated that all zECaC-expressing cells in the skin were MR cells and that only a portion of MR cells expressed zECaC mRNA (Fig. 6, *C* and *D*). Comparing the images of embryos in the same stage (72 hpf), it was noted that MR cells were distributed throughout the entire skin and covering the somites and the yolk (Fig. 6*B*), whereas only the MR cells in the yolk sac skin were expressing zECaC mRNA (Fig. 4*C*).

Whole body Ca^{2+} contents in different developmental stages of embryos. Ca^{2+} contents of zebrafish embryos remained at a constant level (~2 nmol/mg) from 0 to 36 hpf (Fig. 7*A*). The 48-hpf embryos showed a slight increase in the whole body Ca^{2+} content (2.5 nmol/mg), but it did not significantly differ from that of the earlier stages (Fig. 7*A*). Subsequently, embryos

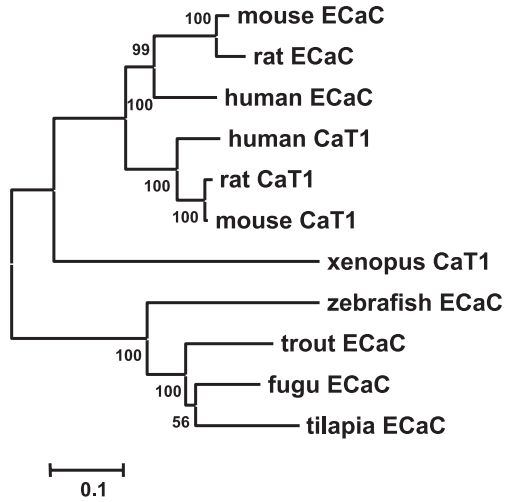

Fig. 2. Phylogenic analysis of vertebrate ECaC amino acid sequences. The consensus tree was generated using the neighbor-joining method with bootstrap analysis using 5,000 replicates. GenBank accession nos. of the sequences used are as follows: mouse ECaC, AF336378; rat ECaC, AB032019; human ECaC, NM_019841; rat Ca^{2+} transporter 1 (CaT1), NM_053686; mouse CaT1, NM_022413; human CaT1, AF365927; *Xenopus* CaT1, AB085630; fugu ECaC, AY232821; and trout ECaC, AY256348. Scale bar represents the uncorrected proportion of amino acid difference.

revealed a growth spurt that was indicated by increasing Ca^{2+} content and enhanced Ca^{2+} influx (see below) for more entry pathway. Whole body Ca^{2+} contents dramatically increased and revealed significant differences at 60 hpf (5 nmol/mg) and 72 hpf (7.5 nmol/mg) (Fig. 7*A*).

Ca^{2+} influx in different developing zebrafish. For the measurement of Ca^{2+} influx, the chorions of fish embryos had to be removed to minimize contamination from the tracer medium. Because dechorionization of 0-hpf embryos is hard to achieve, measurements of Ca^{2+} influx began with 12-hpf embryos. No Ca^{2+} influx was detected in embryos at 12–24 hpf. In 36- and 48-hpf embryos, a significant increase appeared compared with earlier stages (Fig. 7*B*). The Ca^{2+} influx of 60- and 72-hpf individuals continued to increase, and both stages significantly differed from those of the earlier stages (Fig. 7*B*). According to the above results, the Ca^{2+} influx of zebrafish embryos began at 36 hpf, and this was reflected in the whole body Ca^{2+} contents, which started to increase steeply after 48 hpf (Fig. 7, *A* and *B*).

Effects of environmental Ca^{2+} levels on Ca^{2+} influx and zECaC expression. Acclimation to the artificial freshwater containing different levels of Ca^{2+} for 5 days (0–120 hpf) did not cause a significant effect on hatching or survival but did induce significant changes in both Ca^{2+} influx and zECaC expression in developing zebrafish. zECaC mRNA signals in both gills and body skin of the low-Ca^{2+} group were obviously stronger than those of the high-Ca^{2+} group (control) (Fig. 6, *E* and *F*). Ca^{2+} influx and the number, size, and mRNA intensity of the zECaC-expressing cells were significantly higher (~1.7,1.5, 1.9, and 4.3 times higher, respectively) in the low-Ca^{2+} group than in the high-Ca^{2+} group at 120 hpf (Table 1).

DISCUSSION

The ECaC was cloned from zebrafish gills in the present study. The 2,578-bp cDNA encodes a protein of 709 aa, and it shares the highest identity of 73% with the recently cloned rainbow trout ECaC by homology comparison. The identities of the zECaC with other ECaC proteins from mammals were 48–53%. In the case of other transporters, such as the Na^+ pump, the identity between tilapia and mammals exceeds 85% for the α_1- or α_3-subunits (8). The Na^+/K^+-ATPase α-subunits of zebrafish also share 77–92% amino acid identities with the rat α_1-, α_2-, and α_3-subunits, respectively (41). The identities of the ECaC between fishes and mammals are comparatively lower; however, the transmembrane domains and some functionally important residues are all conserved between these species. Similar results also were reported in fugu ECaC (40).

In the phylogenetic tree, trout, fugu, tilapia, and zebrafish ECaCs were clustered together and formed a distinct group from the amphibian and mammalian ECaCs. This indicates that fish and mammalian ECaCs are not orthologous genes and that duplication of the ECaC may have occurred after the divergence of fish and mammals. In the study by Müller et al. (32), gene mapping of two mammalian ECaC isoforms showed that they are both localized on the same chromosome and adjacent to each other, and the authors suggested duplication of a common ancestral gene during evolution. Both phylogeny mapping and chromosome mapping results suggest that there is one gene that encodes the ECaC in zebrafish. The same conclusion was made in fugu (40). To further investigate whether there are two related ECaC genes in the zebrafish genome, we may design different pairs of degenerate primers, which are derived from conserved regions, to amplify genomic fragments in which the intron sizes are different in two mammalian ECaC genes. The reason for the single ECaC gene in zebrafish requires further studies of the ECaC's evolution.

The tissue distribution of the mammalian ECaC and CaT1 has been extensively studied (15, 17, 34, 48). As shown by RT-PCR analysis, the ECaC was expressed mainly in the kidneys, whereas CaT1 expression was distributed in most of the organs, including brain, placenta, ovary, testis, lung, liver, pancreas, kidney, skin, osteoblasts, and the entire gastrointes-

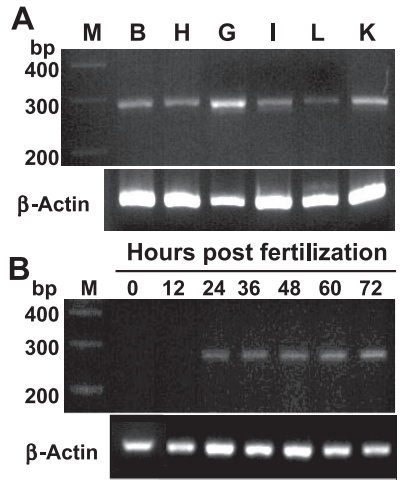

Fig. 3. Zebrafish ECaC (zECaC) expression patterns in various tissues of adults (*A*) and different developmental stages of embryos (*B*) determined by RT-PCR analysis. Zebrafish β-actin was used as the internal control to evaluate the relative amount of cDNA. M, marker; B, brain; H, heart; G, gill; I, intestine; L, liver; K, kidney. The zECaC was ubiquitously expressed in the tissues examined (*A*) and began to be expressed at 24 h postfertilization (hpf) in zebrafish embryos (*B*).

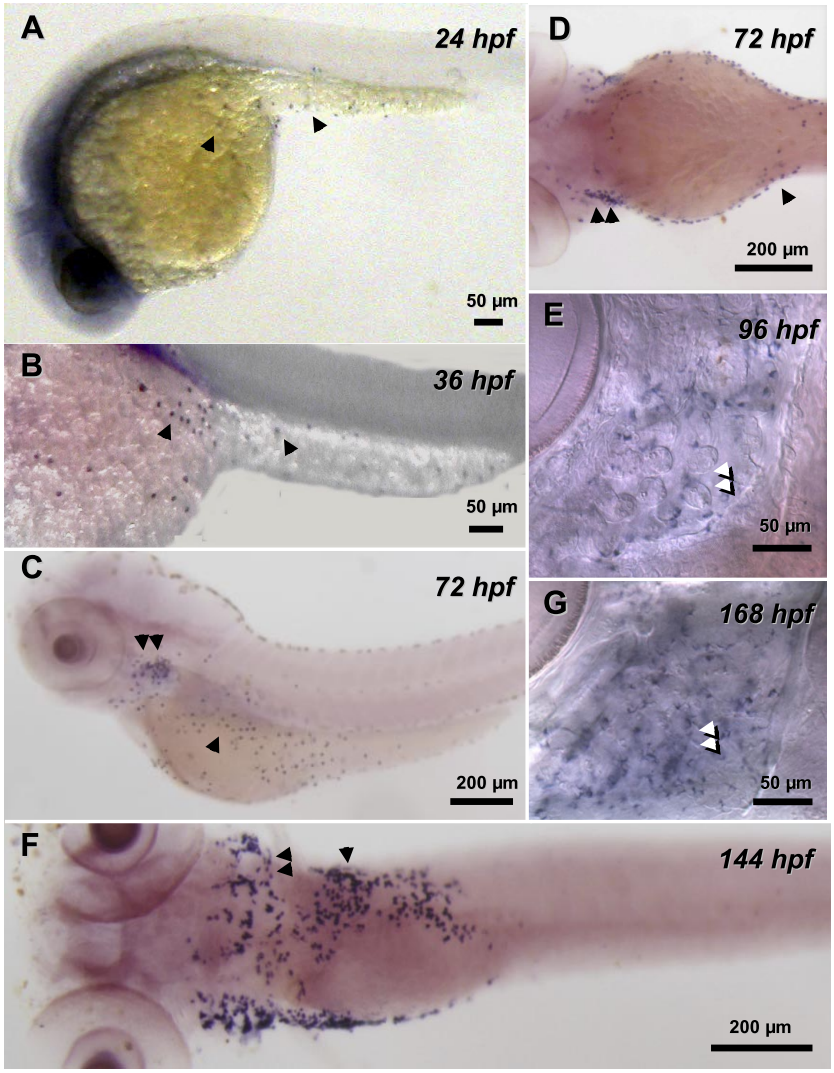

Fig. 4. Whole mount zECaC in situ hybridization of zebrafish embryos at different developmental stages: 24 hpf (*A*), 36 hpf (*B*); 72 hpf (*C* and *D*, ventral view); 96 hpf (*E*); 144 hpf (*F*, ventral view); and 168 hpf (*G*). The zECaC signals (single arrowheads) initially appeared in the skin covering the yolk sac at 24 hpf (*A*). zECaC-expressing cells gradually extended over the entire skin covering the yolk sac (*A–C*) and the branchial area (*C* and *D*, double arrowheads) after development. zECaC-expressing cells began to appear in gill filaments at 96 hpf (*E*), and the cell numbers increased in both the skin (*C* and *F*) and gills (*E–G*) thereafter.

tinal tract (46). In addition to the role of active Ca^{2+} absorption, CaT1 expression in various tissues implied other functions, such as controlling Ca^{2+} entry and intracellular Ca^{2+} concentration in many nonepithelial tissues, cell proliferation and differentiation in keratinocytes (48), and involvement in store-operated Ca^{2+} entry for the signal transduction process (39). In the present study, the zECaC was expressed in the brain, heart, gills, intestines, liver, and kidneys, as shown by RT-PCR analysis. However, in the studies of Hoenderop et al. (17) and Peng et al. (34), ECaC transcripts were only detected in the intestines, kidneys, and placenta with Northern hybridization analysis. Expression levels may be relatively lower in tissues including the brain, heart, and liver, and thus it can only be detected by PCR amplification. Further research is required to determine the exact functions of the zECaC in these nonepithelial tissues. zECaC's expression in gills, intestines, and kidneys is consistent with its role in active Ca^{2+} uptake in mammals, especially the highest expression level in gills, which is considered to be the major site for transcellular Ca^{2+} uptake in fish compared with the intestine (9).

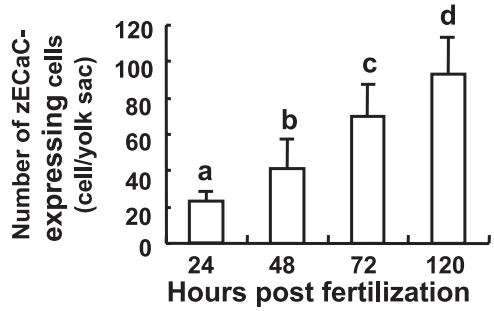

Fig. 5. zECaC expression cell density in yolk sac (cells/yolk sac) at different developmental stages of zebrafish embryos. zECaC-expressing cells in 1 side of the yolk sac were counted. One-way ANOVA was conducted among different embryonic stages. [a,b,c,d]Different letters indicate significant differences between stages (Tukey's pairwise comparison). Values shown are means ± SD; $n = 10$. The cell density in yolk sac increased after zebrafish development.

MR cells have been suggested to be sites for Ca^{2+} uptake in both adult gills and the larval body and yolk sac skins (9, 12, 21, 23, 31, 33); however, no molecular evidence is available so far (36). RT-PCR and in situ hybridization data demonstrate expression of the zECaC in gills and skin of zebrafish; moreover, the mRNA signals were for the first time localized in MR cells with double labeling of Na^+/K^+-ATPase, which is a

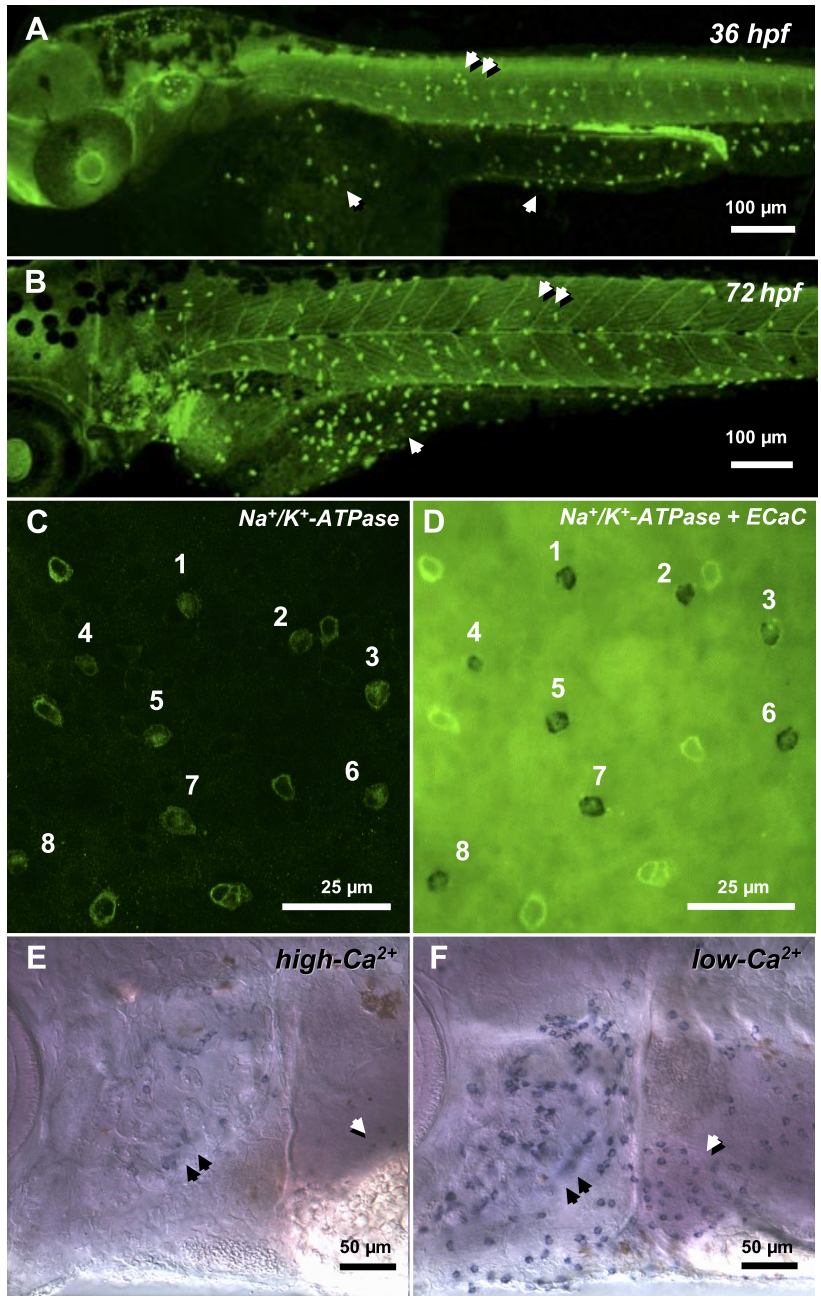

Fig. 6. Images of mitochondria-rich (MR) cells and zECaC-expressing cells. *A* and *B*: MR cells labeled with Na^+/K^+-ATPase in 36- and 72-hpf zebrafish embryos. MR cells appeared through the yolk sac skin (single arrowheads) and body skin (double arrowheads), and the cell number increased after development. *C* and *D*: colocalization of Na^+/K^+-ATPase and zECaC mRNA in 36-hpf zebrafish embryos. Numbers in *C* (Na^+/K^+-ATPase signal only) and *D* (merged image of Na^+/K^+-ATPase and zECaC mRNA signals) indicate the portion of MR cells that expressed zECaC. *E* and *F*: comparison of zECaC expression in 120-hpf zebrafish embryos acclimated to high-Ca^{2+} (*E*) and low-Ca^{2+} freshwater (*F*). zECaC-expressing cells in both gills (double arrowheads) and body skin (single arrowheads) were much more numerous in low-Ca^{2+} (*F*) than in high-Ca^{2+} embryos (*E*).

marker for MR cells. It was noted that only part of the MR cells in zebrafish larval skin expressed the ECaC, and this provides important clues for the existence of functional subtypes of MR cells. Polymorphism of MR cells in fish gills has been well documented to play crucial roles in the uptake of diverse ions as well as in acid-base regulation (4, 28, 36, 38). Pisam et al. (38) identified α and β MR cells in gills of several teleosts and proposed that β MR cells are responsible for Ca^{2+} uptake. In tilapia gills, Tsai and Hwang (43, 44) identified wheat germ agglutinin (WGA; a kind of lectin that can bind to the glycoprotein secreted in the apical region/pit and to the intrinsic glycoprotein of the cells)-positive MR cells and proposed the function of Ca^{2+} uptake. Previously, we identified wavy-convex, shallow-basin, and deep-hole MR cells in tilapia and stenohaline cyprinids according to the apical morphologies and proposed that one of the MR subtype cells (shallow basin) is closely associated with the function of Ca^{2+} uptake, based on serial morphological/physiological studies (4, 27, 28). The present study provides further molecular evidence for these morphological and physiological data concerning the subtypes of MR cells. Only 20–30% of the skin MR cells in zebrafish embryos expressed ECaC mRNA, and these ECaC-expressing MR cells were limited to the skin covering the yolk sac. These data suggest the possibility that at least two subtypes of MR cells differ in their cell distribution (the yolk sac skin vs. the somite skin) and perhaps their functions (Ca^{2+} uptake vs. other ions). We are interested in examining whether the shallow-basin (4), β (39), or WGA-positive MR cells (43) specifically express the ECaC. On the other hand, our unpublished data indicated that the first MR cell opening (another indicator for

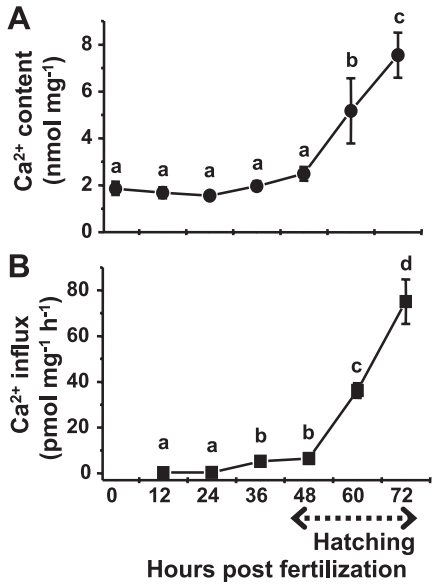

Fig. 7. Ca^{2+} content (*A*) and influx (*B*) at different developmental stages of zebrafish embryos. One-way ANOVA was conducted among different stages. [a,b,c,d]Different letters indicate significant differences between stages (Tukey's pairwise comparison). Values shown are means ± SD; $n = 11$ for content, $n = 6$ for influx. Ca^{2+} content remained at a constant level from 0 to 48 hpf and significantly increased at 60 and 72 hpf (*A*). Ca^{2+} influx began at 36 hpf, followed by a significant increase at 60 and 72 hpf (*B*).

the functional MR cells) was observed in 36-hpf zebrafish embryos, and the density of the MR cell openings was increased about sixfold from 36 to 72 hpf. Our preliminary experiments confirmed that neither concanavalin A nor peanut agglutinin (markers for the apical opening of MR cells) showed specific binding to the MR cells in zebrafish embryos. When and what portion of MR cells with or without ECaC expression in zebrafish embryos is in contact with the outer water remains to be confirmed.

The regulatory mechanisms for Ca^{2+} and other cations during embryonic and larval fish development have been characterized in several papers. Hwang et al. (21) reported that Na^+, K^+, and Ca^{2+} levels remain at constant levels during embryonic stages, followed by a rapid increase after hatching in tilapia. In the same study, Ca^{2+} influx was first detected at 48 hpf and showed a significant increase (from 11.8 to 47.8 $pmol \cdot mg^{-1} \cdot h^{-1}$) after 96 hpf, which corresponds to the hatching time for tilapia larvae. In the study by Chen et al. (5), the Ca^{2+} content of larval zebrafish gradually increased from 0 to 5 days after hatching, and the same pattern occurred for Ca^{2+} influx. In the case of salmon, Ca^{2+} also was acquired from the ambient environment after hatching (14). In the present study, zebrafish hatched during the period of 48 to 72 hpf, and during this same time, both whole body Ca^{2+} content and Ca^{2+} influx showed significant increases. The average Ca^{2+} content in 72-hpf embryos was 7.55 nmol/mg and was about three times higher than that in 0- to 48-hpf embryos, in which Ca^{2+} contents remained at constant levels. Ca^{2+} influx began to increase at 36 hpf, and no influx was detected before that. The time point for Ca^{2+} influx in zebrafish embryos was earlier than that (48 hpf) in tilapia, because the 3-day embryonic stage of zebrafish is shorter than that of tilapia (4 days). A common phenomenon among all species studied is the rapid accumulation of Ca^{2+} after hatching. This implies a definite need for Ca^{2+} uptake from the ambient environment to fulfill the events (e.g., ossification) during larval development, whereas during the embryonic stage, the Ca^{2+} level in oocytes or 0-hpf embryos may be sufficient for the needs of all the developmental processes including cell migration, mitosis, axis formation, segmentation, and body straightening. These physiological data on the ontogeny of Ca^{2+} uptake function in developing zebrafish are further supported by the molecular evidence of the ECaC, one of the major transporters for Ca^{2+} uptake, in the present study. zECaC mRNA was initially detected at 24 hpf, and the first zECaC-expressing MR cell was also found at the same time. Subsequently, Ca^{2+} influx began to increase at 36 hpf, suggesting that a functional protein mediating Ca^{2+} into the embryos may be expressed or that zECaC-expressing MR cells may develop an apical opening (i.e., functional MR cell; Ref. 29) at that time. Thereafter, both the number of zECaC-expressing MR cells and the whole body Ca^{2+} influx increased after embryonic development.

Induction of an increase in the Ca^{2+} transport capacity by acclimation to low-Ca^{2+} environments has been demonstrated in many species and their larval stages, including rainbow trout (38), tilapia (4, 31), goldfish, and ayu (5). The enhanced Ca^{2+} uptake is characterized by modulation in Ca^{2+} influx kinetics (5, 22, 37) and concomitant proliferation of MR cells (or subtype cells) (4, 31, 37, 43). Our previous study on zebrafish embryos (5) indicated that acclimation to 0.02 mM Ca^{2+} (low Ca^{2+}) freshwater induced increases in Ca^{2+} influx and V_{max}, as well as a decrease in K_m, compared with conditions in 2 mM Ca^{2+} (control). The present study further examined the molecular mechanism behind this acclimation process. Upregulation of ECaC expression (in terms of the number, size, and mRNA level of the ECaC-expressing MR cells) and the whole body Ca^{2+} influx were demonstrated in zebrafish embryos acclimated to low-Ca^{2+} freshwater. This also provides further physiological evidence for the role of the ECaC in the fish Ca^{2+} uptake mechanism.

In summary, the zECaC was expressed in a portion of MR cells in skin and gills of developing zebrafish. zECaC mRNA expression was closely correlated with the profile of Ca^{2+} uptake after zebrafish development, and acclimation to low-

Table 1. *Effects of environmental Ca^{2+} levels on whole body Ca^{2+} influx and zECaC mRNA expression in 120-hpf zebrafish*

	Environmental Level [Ca^{2+}]	
	2.00 mM	0.02 mM
Ca^{2+} influx, $pmol \cdot mg^{-1} \cdot h^{-1}$	177.7±42.4	299.3±49.8*
No. of zECaC-expressing cells, cells/4,900 μm^2	13.2±2.4	20.0±3.3*
Size of zECaC-expressing cells, μm^2	35.0±7.4	65.7±9.3*
mRNA in zECaC-expressing cells, arbitrary numerical value	46.3±26.6	197.9±28.4*

Values are means ± SD ($n = 7$–9). A commercial image analysis program (Image-Pro Plus 4.0; Media Cybernetics, Silver Spring, MD) was used to measure the surface area as cell size and the total intensity of hybridization reaction as the mRNA level in each cell. The data from 15 cells were averaged for each individual. zECaC, zebrafish epithelial Ca^{2+} channel; hpf, hours postfertilization. *$P < 0.05$ (Student's *t*-test).

Ca^{2+} freshwater induced upregulation of zECaC mRNA expression and the Ca^{2+} uptake capacity in zebrafish embryos. Taking these findings together, we conclude that the zECaC plays a physiological role in the fish Ca^{2+} uptake mechanism. However, much remains to be done. Direct evidence to demonstrate that the zECaC protein is responsible for Ca^{2+} uptake in fish is still lacking. Further inhibitor or gene gain (or loss)-of-function studies can be conducted to illustrate the function of the ECaC in fish. Stanniocalcin, a hormone that was found to inhibit the permeability to Ca^{2+} of the apical membrane in gills (45), and 1,25-dihydroxyvitamin D_3, a derivative of vitamin D stimulating Ca^{2+} uptake in both freshwater and marine fishes (12, 30), may be candidates for regulating ECaC expression and its function.

GRANTS

This study was supported by grants to P. P. Hwang from the National Science Council (NSC 93-2313-B001-012) and Academia Sinica (Major Group-Research Project), Taiwan, Republic of China.

REFERENCES

1. **Ackermann GE and Paw BH.** Zebrafish: a genetic model for vertebrate organogenesis and human disorders. *Front Biosci* 8: D1227–D1253, 2003.
2. **Alderdice DF.** Osmotic and ionic regulation in teleost eggs and larvae. In: *Fish Physiology*, edited by Hoar WH and Randall DJ. San Diego, CA: Academic, 1988, vol. 11A, p. 163–251.
3. **Briggs JP.** The zebrafish: a new model organism for integrative physiology. *Am J Physiol Regul Integr Comp Physiol* 282: R3–R9, 2002.
4. **Chang IC, Lee TH, Yang CH, Wei YY, Chou FI, and Hwang PP.** Morphology and function of gill mitochondria-rich cells in fish acclimated to different environments. *Physiol Biochem Zool* 74: 111–119, 2001.
5. **Chen YY, Lu FI, and Hwang PP.** Comparisons of calcium regulation in fish larvae. *J Exp Zool* 295A: 127–135, 2003.
6. **Chou MY, Yang CH, Lu FI, Lin HC, and Hwang PP.** Modulation of calcium balance in tilapia larvae (*Oreochromis mossambicus*) acclimated to low-calcium environments. *J Comp Physiol [B]* 172: 109–114, 2002.
7. **Depeche J.** Ultrastructure of the yolk sac and pericardial sac surface in the embryo of the teleost *Poecilia reticulata*. Relation of this study to chloride cells function in embryonic osmoregulation. *Z Zellforsch Mikrosk Anat* 141: 236–253, 1973.
8. **Feng SH, Leu JH, Yang CH, Fang MJ, Hunag CJ, and Hwang PP.** Gene expression of Na^+-K^+-ATPase alpha 1 and 3 subunits in gills of the teleost, *Oreochromis mossambicus,* adapted to different environmental salinity. *Mar Biotech* 4: 379–391, 2002.
9. **Flik G, Fenwick JC, Kolar Z, Mayer-Gostan N, and Wendelaar Bonga SE.** Whole-body calcium flux in cichlid teleost fish *Oreochromis mossambicus* adapted to freshwater. *Am J Physiol Regul Integr Comp Physiol* 249: R432–R437, 1985.
10. **Flik G, Kaneko T, Greco AM, Li J, and Fenwick JC.** Sodium dependent ion transporters in trout gills. *Fish Physiol Biochem* 17: 385–396, 1997.
11. **Flik G, Van Rijs JH, and Wendelaar Bongar SE.** Evidence for high-affinity Ca^{2+}-ATPase activity and ATP-driven Ca-transport in membrane preparations of the gill epithelium of the cichlid fish *Oreochromis mossambicus*. *J Exp Biol* 119: 335–347, 1985.
12. **Flik G, Verbost PM, and Wendelaar Bongar SE.** Calcium transport process in fishes. In: *Cellular and Molecular Approaches to Fish Ionic Regulation*, edited by Wood CM and Shuttleworth TJ. San Diego, CA: Academic, 1995, p. 317–342.
13. **Guggino WB.** Salt balance in embryos of *Fundulus heteroclitus* and *F. bermudae* adapted to seawater. *Am J Physiol Regul Integr Comp Physiol* 238: R42–R49, 1980.
14. **Hayes FR, Darcy DA, and Sullivan CM.** Changes in the inorganic constituents of developing salmon eggs. *J Biol Chem* 163: 621–631, 1946.
15. **Hoenderop JGJ, Hartog A, Stuiver M, Doucet A, Willems PHGM, and Bindels RJM.** Localization of the epithelial Ca^{2+} channel in rabbit kidney and intestine. *J Am Soc Nephrol* 11: 1171–1178, 2000.
16. **Hoenderop JGJ, Nilius B, and Bindels RJM.** Molecular mechanism of active Ca^{2+} reabsorption in the distal nephron. *Annu Rev Physiol* 64: 529–549, 2002.
17. **Hoenderop JGJ, van der Kemp AW, Hartog A, van de Graaf SFJ, van Os CH, Willems PHGM, and Bindels RJM.** Molecular identification of the apical Ca^{2+} channel in 1,25-dihydroxyvitamin D_3-responsive epithelia. *J Biol Chem* 274: 8375–8378, 1999.
18. **Hwang PP.** Distribution of chloride cells in teleost larvae. *J Morphol* 200: 1–8, 1989.
19. **Hwang PP and Hirano T.** Effects of environmental salinity on intercellular organization and junctional structure of chloride cells in early stages of teleost development. *J Exp Zool* 236: 115–126, 1985.
20. **Hwang PP, Lee TH, Weng CF, Fang MJ, and Cho GY.** Presence of Na^+-K^+-ATPase in mitochondria-rich cells in yolk-sac epithelium of larvae of the teleost, *Oreochromis mossambicus*. *Physiol Biochem Zool* 72: 138–144, 1999.
21. **Hwang PP, Tsai YN, and Tung YC.** Calcium balance in embryos and larvae of the freshwater-adapted teleost, *Oreochromis mossambicus*. *Fish Physiol Biochem* 13: 325–333, 1994.
22. **Hwang PP, Tung YC, and Chang MH.** Effect of environmental calcium levels on calcium uptake in tilapia larvae (*Oreochromis mossambicus*). *Fish Physiol Biochem* 15: 363–370, 1996.
23. **Ishihara A and Muyiya Y.** Ultrastructural evidence of calcium uptake by chloride cells in the gills of goldfish, *Carassius auratus. J Exp Zool* 242: 121–129, 1987.
24. **Jones MP, Holliday FGT, and Dunn AEG.** The ultrastructure of the epidermis of larvae of the herring (*Clupea harengus*) in relation to the salinity. *J Mar Biolog Assoc UK* 46: 235–239, 1996.
25. **Kaneko T, Shiraishi K, Katoh F, Hasegawa S, and Hiroi J.** Chloride cells during early life stages of fish and their functional differentiation. *Fish Sci* 68: 1–9, 2002.
26. **Lasker R and Threadgold LT.** "Chloride cells" in the skin of the larval sardine. *Exp Cell Res* 52: 582–590, 1968.
27. **Lee TH, Hwang PP, and Feng SH.** Morphological studies on gill and mitochondria-rich cells in the stenohaline cyprinid teleosts, *Cyprinus carpio* and *Carassius auratus*, adapted to various hypotonic environments. *Zool Stud* 35: 272–278, 1996.
28. **Lee TH, Hwang PP, Lin HC, and Huang FL.** Mitochondria-rich cells in the branchial epithelium of the teleost, *Oreochromis mossambicus*, acclimated to various hypotonic environments. *Fish Physiol Biochem* 15: 513–523, 1996.
29. **Lin LY and Hwang PP.** Activation and inactivation of mitochondria-rich cells in tilapia larvae acclimated to ambient chloride changes. *J Exp Biol* 207:1335–1344, 2004.
30. **Marshall WS and Bryson SE.** Transport mechanisms of seawater teleost chloride cells: an inclusive model of a multifunctional cell. *Comp Biochem Physiol A* 119: 97–106, 1998.
31. **McCormick SD, Hasegawa S, and Hirano T.** Calcium uptake in the skin of a freshwater teleost. *Proc Natl Acad Sci USA* 89: 3635–3638, 1992.
32. **Müller D, Hoenderop JGJ, Meij IC, van der Heuvel LPJ, Knoers NVAM, den Hollander AI, Eggert P, García-Nieto V, Claverie-Martín F, and Bindels RJ.** Molecular cloning, tissue distribution, and chromosomal mapping of the human epithelial Ca^{2+} channel (ECAC1). *Genomics* 67: 48–53, 2000.
33. **Payan P, Mayer-Gostan N, and Pan PKT.** Site of calcium uptake in the freshwater trout gill. *J Exp Zool* 216: 345–347, 1981.
34. **Peng JB, Chen XZ, Berger UV, Vassilev PM, Tsukaguchi H, Brown EM, and Hediger MA.** Molecular cloning and characterization of a channel-like transporter mediating intestinal calcium absorption. *J Biol Chem* 274: 22739–22746, 1999.
35. **Perry SF and Flik G.** Characterization of branchial transepithelial calcium fluxes in freshwater trout, *Salmo gairdneri*. *Am J Physiol Regul Integr Comp Physiol* 254: R491–R498, 1988.
36. **Perry SF, Shahsavarani A, Georgalis T, Bayaa M, Furimsky M, and Thomas SLY.** Channels, pump, and exchangers in the gill and kidney of freshwater fishes: their role in ionic and acid-base regulation. *J Exp Zoolog A Comp Exp Biol* 300: 53–62, 2003.
37. **Perry SF and Wood CM.** Kinetics of branchial calcium uptake in the rainbow trout: effects of acclimation to various external calcium levels. *J Exp Biol* 116: 411–433, 1985.
38. **Pisam M, Le Moal C, Auperin B, Prunet P, and Rambourg A.** Apical structures of "mitochondria-rich" alpha and beta cells in euryhaline fish gill: their behavior in various living conditions. *Anat Rec* 241: 13–24, 1995.
39. **Putney JW Jr.** Channelling calcium. *Nature* 410: 648–649, 2001.

40. **Qiu A and Hogstrand C.** Functional characterisation and genomic analysis of an epithelial calcium channel (ECaC) from pufferfish, *Fugu rubrip*. *Gene* 342: 113–123, 2004.
41. **Rajarao SJR, Canfield VA, Mohideen MPK, Yan YL, Postlethwait JH, Cheng KC, and Levenson R.** The repertoire of Na, K-ATPase α and β subunit genes expressed in the zebrafish, *Danio rerio*. *Genome Res* 11: 1211–1220, 2001.
42. **Shen ACY and Leatherland JF.** Structure of the yolksac epithelium and gills in the early developmental stages of rainbow trout (*Salmo gairdneri*) maintained in different ambient salinities. *Environ Biol Fishes* 3: 345–354, 1978.
43. **Tsai JC and Hwang PP.** The wheat germ agglutinin binding sites and development of the mitochondria-rich cells in gills of tilapia (*Oreochromis mossambicus*). *Fish Physiol Biochem* 19: 95–102, 1998.
44. **Tsai JC and Hwang PP.** Effects of wheat germ agglutinin and colchicine on microtubules of the mitochondria-rich cells and Ca^{2+} uptake in tilapia (*Oreochromis mossambicus*) larvae. *J Exp Biol* 201: 2263–2271, 1998.
45. **Van der Heijden AJH, Verbost PM, Bijvelds MJC, Atsma W, Wendelaar Bongar SE, and Flik G.** Effects of sea water and stanniectomy on branchial Ca^{2+} handling and drinking rate in eel (*Anguilla anguilla* L.). *J Exp Biol* 202: 2505–2511, 1999.
46. **Weber K, Erben RG, Rump A, and Adamski J.** Gene structure and regulation of the murine epithelial calcium channel ECaC1 and 2. *Biochem Biophys Res Commun* 289: 1287–1294, 2001.
47. **Wilkinson DG.** In situ hybridization. In: *Essential Development Biology. A Practical Approach*, edited by Stern CD and Holland PWH. Oxford, UK: IRL, 1993, p. 257–276.
48. **Zhuang L, Peng JB, Tou L, Takanaga H, Adam RM, Hediger MA, and Freeman MR.** Calcium-selective ion channel, CaT1, is apically localized in gastrointestinal tract epithelia and is aberrantly expressed in human malignancies. *Lab Invest* 82: 1755–1764, 2002.